Bi-allelic *ADARB1* Variants Associated with Microcephaly, Intellectual Disability, and Seizures

Tiong Yang Tan,[1,2,3,17,*] Jiří Sedmík,[4,17] Mark P. Fitzgerald,[5,16,17] Rivka Sukenik Halevy,[6,7] Liam P. Keegan,[4] Ingo Helbig,[5,16] Lina Basel-Salmon,[6,7,8] Lior Cohen,[9] Rachel Straussberg,[7,10] Wendy K. Chung,[11] Mayada Helal,[11] Reza Maroofian,[12] Henry Houlden,[12] Jane Juusola,[13] Simon Sadedin,[1,2] Lynn Pais,[14] Katherine B. Howell,[2,3,15] Susan M. White,[1,2,3] John Christodoulou,[1,2,3] and Mary A. O'Connell[4,*]

The RNA editing enzyme ADAR2 is essential for the recoding of brain transcripts. Impaired ADAR2 editing leads to early-onset epilepsy and premature death in a mouse model. Here, we report bi-allelic variants in *ADARB1*, the gene encoding ADAR2, in four unrelated individuals with microcephaly, intellectual disability, and epilepsy. In one individual, a homozygous variant in one of the double-stranded RNA-binding domains (dsRBDs) was identified. In the others, variants were situated in or around the deaminase domain. To evaluate the effects of these variants on ADAR2 enzymatic activity, we performed *in vitro* assays with recombinant proteins in HEK293T cells and *ex vivo* assays with fibroblasts derived from one of the individuals. We demonstrate that these ADAR2 variants lead to reduced editing activity on a known ADAR2 substrate. We also demonstrate that one variant leads to changes in splicing of *ADARB1* transcript isoforms. These findings reinforce the importance of RNA editing in brain development and introduce *ADARB1* as a genetic etiology in individuals with intellectual disability, microcephaly, and epilepsy.

Introduction

The adenosine deaminases acting on RNA (ADARs) are a family of enzymes that catalyze the hydrolytic deamination of adenosine to inosine in double-stranded RNA (dsRNA) (for review, see Sinigaglia et al.[1]). The editing and RNA-binding activities of ADARs affect different aspects of RNA processing and can also lead to RNA recoding because inosine is usually recognized as guanosine by the translation machinery.[2] Three members of the ADAR family, ADAR1, ADAR2, and ADAR3, (encoded by the *ADAR* [MIM: 146920], *ADARB1* [MIM: 601218], and *ADARB2* [MIM: 602065] genes, respectively), have been identified in humans, but only ADAR1 and ADAR2 are enzymatically active. All ADARs contain the eponymous deaminase domain and several double-stranded RNA-binding domains (dsRBDs). ADARs can assemble into heterodimers and homodimers, and the dimerization is important for editing activity.[3–7]

Editing by ADAR1 is essential for innate immunity. Bi-allelic or, rarely, *de novo* heterozygous variants in the encoding gene, *ADAR*, cause Aicardi-Goutières syndrome type 6 (AGS6; MIM: 615010), a genetically heterogeneous interferonopathy characterized by features resembling congenital viral infections, including microcephaly, intellectual disability, brain calcification, dystonia, and high interferon levels.[8,9] Heterozygous variants in *ADAR* have also been reported in association with dyschromatosis symmetrica hereditaria (DSH; MIM: 127400), a macular pigmentary cutaneous condition affecting the face and dorsal extremities.[10] Individuals with features clinically overlapping both AGS and DSH are rare.[11,12]

ADARB1 (GenBank: NM_001112.4) encodes two major protein isoforms of ADAR2: the shorter ADAR2S (ADAR2a; UniProt ID: P78563-2) and longer ADAR2L (ADAR2b; UniProt: P78563-1), which differ by the alternatively spliced exon 5a encoding a flexible RNA-binding loop on the deaminase domain. This alternatively spliced exon extends the deaminase domain of ADAR2L by 40 amino acids. Both ADAR2 isoforms are expressed in the human brain at different developmental stages.[13,14] ADAR2L is less enzymatically active than ADAR2S,[15,16] although *in vitro* editing assays performed with rat ADAR2, which has similar alternative isoforms, demonstrate that the editing efficiencies of the two isoforms at some editing sites is identical.[17]

In general, ADAR2 performs site-specific editing, whereas ADAR1 mediates promiscuous editing of transcripts containing repetitive elements, such as *Alu* elements, that can form intramolecular RNA duplexes.[18] In

[1]Victorian Clinical Genetics Services, Melbourne 3052, Australia; [2]Murdoch Children's Research Institute, Melbourne 3052, Australia; [3]Department of Pediatrics, University of Melbourne, Melbourne 3052, Australia; [4]Central European Institute of Technology, Masaryk University, Kamenice 735/5, A35, Brno 62500, Czech Republic; [5]Division of Neurology, Departments of Neurology and Pediatrics, The Children's Hospital of Philadelphia and the Perelman School of Medicine at the University of Pennsylvania, Philadelphia, PA 19104, USA; [6]Raphael Recanati Genetic Institute, Rabin Medical Center-Beilinson Hospital, Petah Tikva 49100, Israel; [7]Sackler Faculty of Medicine, Tel Aviv University, Tel Aviv 6997801, Israel; [8]Felsenstein Medical Research Center, Petah Tikva 49100, Israel; [9]Pediatric Genetics Unit, Schneider Children's Medical Center of Israel, Petah Tikva 49100, Israel; [10]Pediatric Neurology Unit, Schneider Children's Medical Center of Israel, Petah Tikva 49100, Israel; [11]Department of Pediatrics, Columbia University Medical Center, New York, NY 10032, USA; [12]Department of Neuromuscular Disorders, University College London Queen Square Institute of Neurology, London WC1N 3BG, UK; [13]GeneDx, Gaithersburg, MD 20877, USA; [14]Broad Center for Mendelian Genomics, Broad Institute of MIT and Harvard, Cambridge, MA 02142, USA; [15]Department of Neurology, Royal Children's Hospital, Parkville 3052, Australia; [16]The Epilepsy NeuroGenetics Initiative, Children's Hospital of Philadelphia, Philadelphia, PA 19104, USA
[17]These authors contributed equally to this work
*Correspondence: mary.oconnell@ceitec.muni.cz (M.A.O.), tiong.tan@vcgs.org.au (T.Y.T.)
https://doi.org/10.1016/j.ajhg.2020.02.015.

humans, adenosine-to-inosine (A-to-I) editing resulting in recoding in exons is rare and predominantly occurs in the brain within transcripts encoding subunits of neuroreceptors and ion channels. Editing can modulate the properties of encoded neuronal proteins. One of the best-studied transcripts recoded by ADAR2 is *Gria2*, which encodes a subunit of the ionotropic α-amino-3-hydroxy-5-methyl-4-isoxazolepropionic acid (AMPA) receptor. The adenosine at the Q/R site of *Gria2* is edited in up to 100% of transcripts, resulting in a change of a glutamine (Q) codon to arginine (R). This change leads to AMPA receptors being impermeable to calcium[19] and decreases trafficking of the assembled AMPA receptor from the endoplasmic reticulum to the postsynaptic region.[20,21] The net effect of a reduction in RNA editing of the mouse *Gria2* Q/R site is an increase in the calcium permeability of AMPA receptors and an increase in their number at the postsynaptic region. A recent study reported 28 individuals who had intellectual disability and neurodevelopmental abnormalities and who also had *de novo* heterozygous variants in *GRIA2* (MIM:138247). One of the most deleterious variants, p.Gln607Glu, occurred at the Q/R site in an individual with a severe epileptic encephalopathy. The resulting gain-of-function increase in channel current reinforces the importance of this editing site[22] However, other editing substrates of ADAR2 or editing-independent functions of ADAR2 could also play a role in brain physiology.

Herein we report on four unrelated individuals with bi-allelic *ADARB1* variants associated with microcephaly, intellectual disability, and seizures, which were intractable in three of the individuals. We observed reductions in ADAR2 editing activity with four of the five variants and no changes in ADAR2 localization as assayed *in vitro* with recombinant proteins expressed in cultured cells. One of the variants, c.1808G>A (p.Arg603Gln), appears to affect the stability of recombinant ADAR2. Another variant, c.1492A>G (p.Thr498Ala), alters the ratio of two splicing isoforms of the *ADARB1* transcript in two tested cell lines and in fibroblasts derived from the affected individual. These data suggest that bi-allelic variants in *ADARB1* cause microcephaly, intellectual disability, and intractable epilepsy, reinforcing the importance of RNA editing in human brain development.

Subjects and Methods

We use the *ADARB1* exon numbering proposed by Slavov and Gardiner.[23] On the basis of this numbering, the Alu-J cassette exon of ADAR2L is referred to as exon 5a. The numbering of amino acids in this paper is based on the longer protein isoform ADAR2L.

Participant Recruitment and Sequencing

Individuals were clinically evaluated in separate centers, and contact between researchers was facilitated by use of the web-based tools Matchmaker Exchange[24] and GeneMatcher.[25] Individual 1 underwent trio exome sequencing by the Genomics Platform at the Broad Institute of Harvard and MIT (Broad Institute, Cambridge, MA, USA)[26] as part of the Murdoch Children's Research Institute Undiagnosed Diseases Project (RCH HREC 36291A), individual 2 underwent exome sequencing through GeneDx (Gaithersburg, MD) on a clinical basis, individual 3 underwent trio exome sequencing as part of a pilot program funded by the Israeli Ministry of Health, and Individual 4 underwent trio exome sequencing as described by Zhu et al.[27]

Cell Culture

HEK293T cells were cultured in MEM with Earle's Salts (biosera) supplemented with non-essential amino acids (Sigma-Aldrich), 10% fetal calf serum (FCS), and penicillin-streptomycin (biosera). SH-SY5Y cells were cultured in Ham's F12 medium and MEM with Earle's Salts (mixed 1:1, biosera) supplemented with non-essential amino acids, 15% FCS, and penicillin-streptomycin. HeLa cells were cultured in DMEM High-Glucose (biosera) supplemented with non-essential amino acids, 10% FCS, and Penicillin-Streptomycin. Fibroblasts were cultured in high-glucose DMEM (biosera) supplemented with non-essential amino acids, 15% FCS, and penicillin-streptomycin. All the cell lines were grown as monolayers at 37°C with 5% CO_2.

Plasmid Constructs and Site-Directed Mutagenesis

Phusion Hot Start II polymerase (Thermo Fisher) was used for all cloning and mutagenesis PCRs. We amplified the full-length ADAR2 coding sequence from HeLa cDNA by using PCR with gene-specific primers introducing N-terminal FLAG-tag and C-terminal 6xHis-tag (both tags were separated by two residues, Leu and Val, from the coding sequence). We used a second pair of primers to introduce *att*B Gateway Cloning sites. ADAR2S and ADAR2L bands were cut out and extracted from agarose gel and cloned into a pc3D destination vector[28] with Gateway Cloning (Thermo Fisher). The plasmid expressing human *pri-mir-376a2* RNA editing substrate was generated previously.[28] For the splicing assay, primers with *att*B cloning sites were designed to amplify a minigene that contains exons 5, 5a, and 6 of human *ADARB1* from HEK293T gDNA, and the PCR product was cloned into pDESTsplice destination vector[29] with Gateway Cloning. For mutagenesis, ADAR2 wild-type (WT) plasmids were used as templates for amplification with primers containing the desired variants. The PCR products were treated with *Dpn*I restriction enzyme (Thermo Fisher) at 37°C for 1 h and transformed into *E. coli* DH5α or TOP10 strains.

Transient Transfection

For the editing assay, HEK293T cells were seeded on 12-well plates 24 h before transfection at ~73,500 cells/cm^2 (255,000 cells per well). 1 μg of *ADARB1* expressing plasmid and 1 μg of the editing reporter plasmid were mixed with 3.5 μl of Lipofectamine 3000 (Thermo Fisher) and used for co-transfection as per the manufacturer's instructions. Cells were collected 72 h after transfection by gentle washing with PBS and divided into two tubes. The cell pellet from one tube was used for RNA extraction with TriPure reagent (Sigma-Aldrich), whereas the other cell pellet was used for immunoblotting.

For the cycloheximide chase assay, the seeding of HEK293T cells on 12-well plates was performed as for the editing assay. 1 μg of *ADARB1*-expressing plasmid and 2.5 μl of Lipofectamine 3000 were used for transfection as per the manufacturer's instructions. 24 h after transfection, cells were either treated with 70 μg/mL of cycloheximide (Sigma-Aldrich) for indicated times or left untreated. Cells were collected 48 h after the transfection, and the cell pellet

was used for immunoblotting. The densitometric analysis of immunoblots was performed with Image Studio Lite program (LI-COR).

For the splicing assay, SH-SY5Y cells and HeLa cells were seeded on six-well plates 24 h before transfection at ~42,100 cells/cm^2 (400,000 cells per well) or at ~29,500 cells/cm^2 (280,000 cells per well), respectively. 2 μg of *ADARB1* minigene plasmid with 3 μl (HeLa) or 4 μl (SH-SY5Y) of Lipofectamine 3000 were used for transfection as per the manufacturer's instructions. We collected cells 24 h after transfection by adding 750 μl of TriPure reagent directly to plates.

Immunofluorescence

HeLa cells were seeded on coverslips coated with 0.2% gelatin in 24-well plates at ~26,800 cells/cm^2 (50,000 cells per well). The cells were transfected at the time of seeding with 500 ng of *ADARB1*-expressing plasmid and 0.75 μl of Lipofectamine 3000 per well, as per the manufacturer's instructions. All of the following steps were performed at room temperature. After 24 h, the coverslips were briefly rinsed in PBS, fixed in 3.7% formaldehyde (diluted in PBS) for 10 min, and quenched with 50 mM NH_4Cl (diluted in PBS) for 5 min. The cells were then washed with PBS and permeabilized with 0.2% Triton X-100 for 5 min. The coverslips were washed again with PBS and blocked with blocking solution (1% BSA + 0.05% Tween 20) for 60 min. Staining was performed with rabbit anti-FLAG polyclonal antibody (F7425, Sigma-Aldrich) diluted 1:800 in blocking solution for 60 min. After the staining, the coverslips were washed three times in PBS + Tween 20 (PBST) and stained with Alexa Fluor 568 goat anti-rabbit IgG (H+L) polyclonal secondary antibody (A-11011, Thermo Fisher) diluted 1:200 in PBS with 0.3 μg/mL DAPI for 60 min. The coverslips were then washed twice in PBST and once in PBS, rinsed with Milli Q water and mounted in Mowiol 4-88 mounting medium (EMD Millipore). Samples were analyzed with an inverted microscope Zeiss Axio Observer.Z1 with a confocal unit LSM 800 or with an upright microscope Zeiss AxioImager.Z2.

Immunoblotting

The cell pellet was resuspended in 15 μl of lysis buffer (10 mM Tris-HCl [pH 8], 10 mM EDTA [pH 8], 0.1 M NaCl, and 2% SDS) with 1x cOmplete Protease Inhibitor (Roche) added and lysed for 30 min at 4°C. Whole-cell lysate was pelleted by centrifugation, and the clear supernatant was used for immunoblotting. Lysates were boiled for 5 min in Laemmli buffer prior to electrophoretic separation on 8% or 10% SDS polyacrylamide gel and blotting on a nitrocellulose membrane. Antibodies used for immunoblots are listed in the Supplemental Information.

RNA Extraction and Reverse Transcription

Total RNA was isolated with TriPure reagent according to the manufacturer's instructions. RNA samples were treated with 10 U of DNase I (Roche) per 50 μg of total RNA and then purified by phenol-chloroform extraction and ethanol precipitation with sodium acetate. A 2.0–2.5 μg aliquot of DNase-treated total RNA was reverse transcribed into cDNA with RevertAid RT Kit (Thermo Fisher) according to the manufacturer's instructions; 2.5 μM of oligo(dT)$_{18}$ (fibroblasts) or 0.25 μM of both *GAPDH* Rv and *ADARB1* exon 5a splicing reporter Spl2 primers (SH-SY5Y and HeLa) were used.

Real-Time PCR

All quantitative PCR experiments were performed with a LightCycler 480 Instrument II (Roche). PCR was performed with LightCycler 480 SYBR Green I Master (Roche) with the following cycling conditions: 1 cycle of 95°C for 10 min, then 45 cycles of 95°C for 10 s, 60°C for 20 s, and 72°C for 10 s. Gene-specific primers used for PCR amplification are summarized in Table S1. All samples were tested in technical duplicates and normalized to *GAPDH*. The relative expression of target genes was calculated with the $2^{-\Delta\Delta CT}$ method.[30] Biological quadruplicates were used for calculating the mean and standard deviation. Statistical significance of differences between samples was determined by two-tailed t tests with Microsoft Excel.

Data Availability

The authors confirm that the data supporting the findings of this study are available within the article and its supplemental information.

Results

Clinical Phenotypic Characterization

Affected individuals were microcephalic at birth (individual 1) or developed postnatal microcephaly ranging from −3.6 to −4.0 SD, experienced seizures, and had either severe global developmental delay or intellectual disability. The affected children do not share a specific facial gestalt (Figures 1A–1E). All four had severe feeding difficulties, and two required percutaneous endoscopic gastrostomy (PEG) feeds. Neuroimaging of individuals 1–4 demonstrated various non-specific abnormalities, including thinning of the corpus callosum, delayed myelination, and cerebral atrophy, but no calcifications (Figures 1F–1K). No cutaneous abnormalities, such as chilblains, were identified in any of the affected individuals at their most recent evaluations. Salient features are described here, and more detailed descriptions are summarized in Table 1 and Supplemental Information.

Individual 1 is one of two children born to healthy non-consanguineous Australian parents of European descent. Developmental delay and hypotonia were present in individual 1 from infancy. His head circumference at birth was 30.5 cm (−2.2 SD), but this worsened in infancy such that it now tracks at −3.4 SD. At age 4 years, he needed help to stand and was unable to walk independently. He has limited intelligible speech but vocalizes and understands some sign language. At age 5 years, he had his first generalized tonic-clonic seizure. He also has frequent staring spells not considered to be absence episodes. His EEG showed a slow and less well-modulated background for his age, but no epileptiform activity.

The parents of individual 2 are healthy non-consanguineous individuals of Hispanic descent. Individual 2 experienced infantile-onset focal clonic and tonic-clonic seizures that were intractable to multiple therapies, including phenobarbital, levetiracetam, oxcarbazepine, topiramate, pyridoxine, pyridoxal-5-phosphate, phenytoin, lacosamide, clonazepam, clobazam, rufinamide, valproic acid, felbamate, the ketogenic diet, quinidine, and vagal nerve stimulation. Individual 2 died from epilepsy at the age of 2 years. Prior to his death, his development was

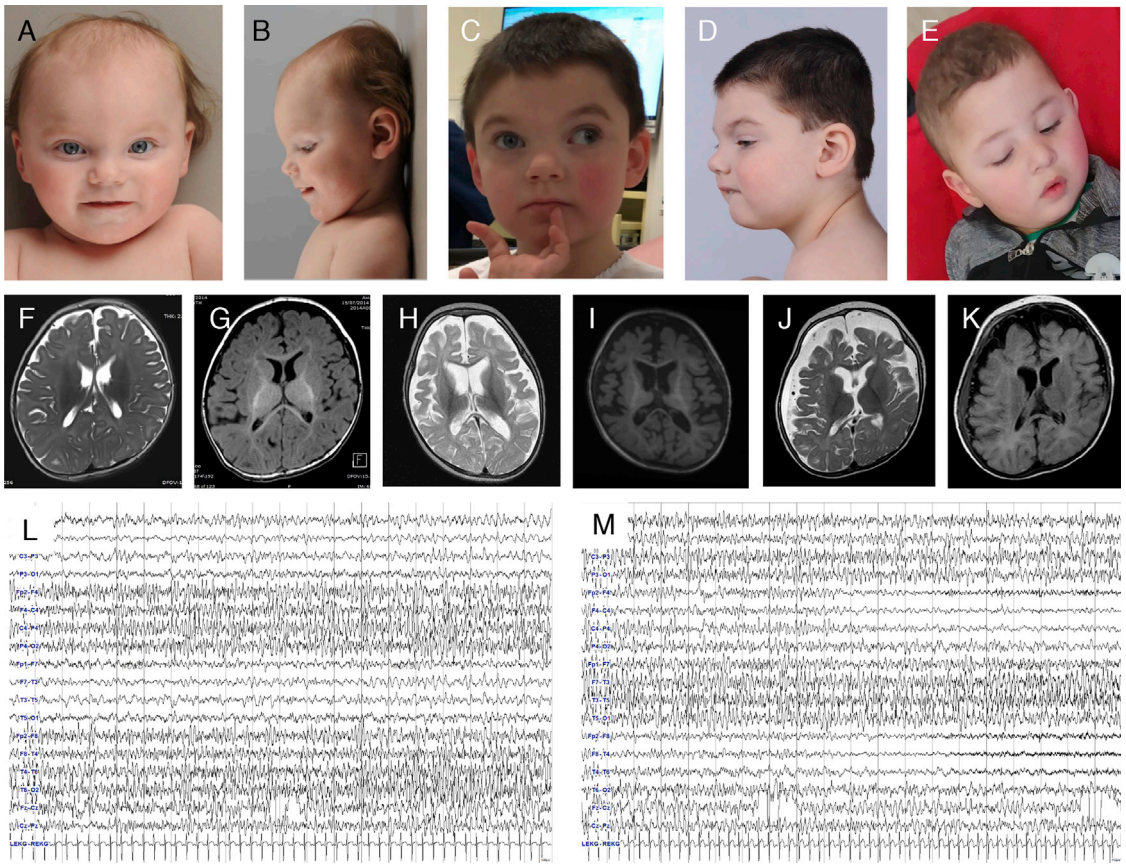

Figure 1. Clinical and Neuroradiographic Images of Individuals 1–3.
(A and B) Frontal (A) and lateral (B) image of individual 1 at age 10 months; note plagiocephaly.
(C and D) Frontal (C) and lateral (D) image of individual 1 at 4 years, 4 months; note the exotropia but general lack of dysmorphic features.
(E) Frontal image of individual 3 at 2 years; note the lack of dysmorphic features.
(F–K) Axial T2 (F, H, and J) and T1 (G, I, and K) weighted MRI images from individual 1 at 6 months of age (F and G), individual 2 at 22 months of age (H and I), and individual 3 at 23 months of age (J and K) demonstrate cerebral volume loss and thinning of the corpus callosum.
(L and M) An EEG of individual 2 demonstrates migrating focal seizures. Image L demonstrates a right hemispheric electrographic seizure, shereas image M, taken 15 s later, demonstrates the right hemispheric seizure ending while an independent left hemispheric seizure evolves.

profoundly delayed. He was unable to visually track objects, roll over, or sit, and he never achieved head control or meaningful language. His neurological examination was remarkable for microcephaly and included plagiocephaly, severe hypotonia, cortical blindness, and limited voluntary movement. Individual 2's seizure semiology and EEG were consistent with epilepsy of infancy with migrating focal seizures (Figures 1L and 1M).

Individual 3 is a 2-year-old boy born to consanguineous parents. He presented with severe developmental delay and intractable seizures that began at age 4 months, at which time antiepileptic treatment (levetiracetam, phenobarbital, topiramate, pyridoxine, and a ketogenic diet) began. An EEG at the age of 8 months showed epileptic foci in the left temporal and occipital regions, but a sleep EEG at 18 months recorded no epileptic activity. At age 2 years, individual 3 had not achieved any developmental milestones; he was inactive, poorly responsive, made no eye contact, and did not interact with his surroundings.

Individual 4 is an 11-year-old boy born to first-cousin Azari parents. Developmental delay was noted in the first months of life, and generalized intractable seizures began at age 7 months, after which he experienced developmental stagnation. An EEG at the age of 9 years demonstrated both focal and generalized epileptiform discharges. At age 11 years, he has failure to thrive, feeding difficulties, profound intellectual disability, microcephaly, and ongoing generalized tonic-clonic seizures treated with carbamazepine. He is non-verbal, non-ambulatory, does not visually fix, and has central hypotonia and peripheral hypertonia. He has repetitive movements of his left hand and neck.

Exome Sequencing Results

All four individuals were found to have bi-allelic missense variants in *ADARB1* (see Table 2 for variant details). All clinically unaffected parents and siblings are either heterozygous carriers or homozygous for the reference allele.

Table 1. Clinical Phenotype of Affected Individuals

Patient ID	Individual 1	Individual 2	Individual 3	Individual 4
Gender	male	male	male	male
Age at last examination	5 years, 9 months	24 months (deceased)	2 years	11 years
Phenotype				
Prenatal and neonatal history	concern about CMV infection in first trimester; but no CMV detected by PCR of amniotic fluid, neonatal blood and urine; neonatal jaundice treated with 3 days of phototherapy	c-section due to pre-eclampsia; no other complications with pregnancy or delivery. Spent 7 weeks in NICU, not intubated; had anemia requiring blood transfusion and had apnea requiring caffeine.	during the pregnancy elevated Nuchal translucency (3.8 mm) microcephaly and polyhydramnios (AFI-27 CM) were detected	no complications during pregnancy or delivery
Prenatal structural anomalies	no	no	elevated nuchal translucency (3.8 mm) microcephaly and polyhydramnios (AFI-27 CM)	no
Gestational age at birth	40	31	40	38
Congenital abnormalities	no	no	yes	no
Growth (age)				
Most recent height in cm (SD)	100 cm (−1.3 SD)	81 cm (−2 SD)	76 cm (−3.6 SD)	114 cm (−4.3 SD)
Most recent weight in kg (SD)	15.5 kg (−0.8 SD)	10.95 kg (−0.9 SD)	unknown	20 kg (−4.1 SD)
Most recent head circumference in cm (SD)	46 cm (−3.6 SD)	43.5 cm (−4.0 SD)	43 cm (−4.4 SD)	49 cm (−3.3 SD)
Length at birth in cm (SD)	51 cm (+0.5 SD)	unknown	unknown	50 cm (−4.3 SD)
Weight at birth in g (SD)	3430 g (+0.17 SD)	1701 g	3500 g	3600 g (+0.51 SD)
Head circumference at birth in cm (SD)	30.5 cm (−2.2 SD)	unknown	36.5 cm (+0.38 SD)	unknown; recalled within normal range
Development				
Motor delay	yes	yes	yes	yes
Age at walking	N/A; can stand with assistance	N/A; unable to roll over or support head	N/A	N/A
Age at first words	12 months	nonverbal	nonverbal	nonverbal
Number of words at most recent evaluation	two	none	none	none
Intellectual disability	yes	yes	yes	yes
Degree of intellectual disability	severe	profound	severe	profound
Neurologic and Psychiatric Features				
Neurological abnormalities	epilepsy, global developmental delay, intermittent tremor in leg	epilepsy, global developmental delay, diffuse hypotonia, symmetric antigravity movements of limbs	epilepsy, global developmental delay, hypertonia with significant spasticity.	epilepsy, global developmental delay, axial hypotonia with appendicular hypertonia and distal contractures, muscle atrophy, repetitive movements of right hand and neck

(*Continued on next page*)

Table 1. ***Continued***

Patient ID	Individual 1	Individual 2	Individual 3	Individual 4
Neuroimaging	MRI (6 months): thin corpus callosum, incomplete myelination; CT (16 months): no calcification, no sutural synostosis	MRI (22 months): microcephaly, diffuse supratentorial volume loss, white matter gliosis, and delayed myelination	MRI (23 months): thin corpus callosum	MRI (3 years): brain atrophy in temporal lobes
EEG findings	slow and less well-modulated background for age, but no epileptiform activity	multifocal epileptiform discharges	focal epileptiform discharges in the left temporal and occipital regions	focal and generalized epileptiform discharges
Seizure semiology	two generalized tonic-clonic seizures	migrating focal seizures	intractable generalized seizures	intractable generalized seizures started at the age of 7 with increased frequency from once a month to once every 15 days
Behavioral problems	no	no	no	no
Sleep disturbance	frequent waking during night; early morning waking	no	no	no
Facial Features				
	round face with metopic ridging, brachycephaly, upslanting palpebral fissures, normal corneal reflexes, thin upper lip	non-dysmorphic with plagiocephaly	oval face with plagiocephaly and high arched palate	non-dysmorphic
Miscellaneous				
Hearing	normal	normal	normal	normal
Vision	exotropia but normal vision	cortical blindness	cortical blindness	cortical blindness
Abnormality of the heart	no	no	no	no
Abnormality of the respiratory system	laryngomalacia	grade 1 subglottic stenosis	no	no
Abnormality of the gastrointestinal system	PEG feeds	PEG feeds	feeding difficulties	feeding difficulties
Abnormality of the urogenital system	no	no	left cryptorchidism	no
Abnormality of the skin / hair / nails	high anterior hairline, sparse scalp hair; no chillblains	no	single café au lait spot on back	no
Abnormality of the musculoskeletal system	no	no	no	no
Abnormality of the endocrine system	no	no	no	no
Abnormality of the immunological system	no	no	no	no
Family History				
Consanguinity	no	no	yes	yes
Miscarriages	no	unknown	Yes; 5 spontaneous early miscarriages	no
Congenital abnormalities	no	no	mother with congenital heart defect	no

(*Continued on next page*)

Table 1. ***Continued***

Patient ID	Individual 1	Individual 2	Individual 3	Individual 4
Intellectual disability	no	no	yes (Supplemental Information)	no
Other	no	high cholesterol (parents)	yes (Supplemental Information)	no
Previous genetic testing				
Karyotype	no	yes,normal	no	yes, normal
Fragile X	yes, normal	no	no	no
Array-CGH	yes, normal	yes, normal	normal	no
Gene-panel testing	no	yes; normal infantile epilepsy panel (genes tested: *ARX, CDKL5, SLC25A22, STXBP1, SPTAN1, SCN1A, GABRG2, KCNQ2, ARHGEF2, PCDH19, PNKP, SCN2A, PLCB1, GABRD, and MEF2C*)	no	no

Four of the five variants reported here are observed in a heterozygous state at low allele frequencies, and none were found in a homozygous state in the gnomAD or epi25 databases (accessed September 24, 2019). In the epi25 database, we did not find any individual compound heterozygous for any combination of the five variants from this cohort. The c.379A>G (p.Lys127Glu) variant is not listed in these databases; only a synonymous variant (rs1210305864) that affects the same codon has been observed previously. No other non-synonymous variants affecting Lys127, Lys367, Thr498, Arg603, or Ala722 were reported.

The Location and Conservation of *ADARB1* Variants

Four of the five *ADARB1* variants identified in the individuals in this cohort lead to ADAR2 amino acid changes situated in or around the deaminase domain, and one is situated in dsRBD1 (Figure 2A). The variant in dsRBD1, p.Lys127Glu, affects a lysine residue that contacts the sugar-phosphate backbone of dsRNA (Figure 2B).[31] The p.Lys367Asn variant is located in strand β2 of the deaminase domain, but the affected lysine lies at the surface of the protein and does not appear to make any contact with other residues in the deaminase domain (Figure 2C). The p.Thr498Ala variant is located in the 40-amino-acid-long in-frame insertion that occurs in the deaminase domain and that is incorporated only in the longer protein isoform ADAR2L. This insertion is encoded by exon 5a, and it extends the RNA-binding loop between strands β5 and β6.[32] The p.Arg603Gln variant is situated near the C-terminal part of helix α7 of the deaminase domain. Arg603 makes contacts with the Cα carbonyls of Gly518 and Ala599 and with the side chain of Asp558 (Figure 2D). The p.Ala722Val variant lies at the surface of the protein and affects the Ccap residue of a Schellman loop at the C-terminal end of helix α10 (Figure 2E).[33]

The importance and conservation of the Lys127 residue from dsRBD1 has been previously established.[34] The multiple-sequence alignment of ADAR family proteins reveals that Lys367 is conserved in mammalian ADAR2 and in dADAR from *Drosophila melanogaster*. On the other hand, Arg603 is highly conserved across the whole ADAR family (Figure 2F). Moreover, Arg603 might be important for deaminase-domain-containing proteins in general because the alignment of various human and mouse deaminases also confirms its conservation, and Asp558, which makes contacts with Arg603, is also conserved (Figure 2G). However, it should be noted that we have lower confidence in the fidelity of the alignment in Figure 2G because the sequence around Arg603 is not as conserved as in other highly conserved regions (e.g., Arg562 and Lys669, which interact with IP6) and because of the presence of gaps in the aligned ADAD1 sequence; both of these allow for multiple alignment possibilities. Ala722 is highly conserved in ADAR2 and ADAR3, except for in *Xenopus tropicalis* and *Takifugu rubripes* (Figure 2F). Because exon 5a, where the Thr498 residue is located, originates from a primate-specific *Alu* element inserted in *ADARB1* sequence, most of the sequences have a gap in the alignment at this position (Figure S1).

The ADAR2 Variants p.Lys127Glu, p.Lys367Asn, p.Arg603Gln, and p.Ala722Val Result in Decreased Editing Activity of ADAR2

To test the initial hypothesis that the *ADARB1* variants would cause a decrease in ADAR2 editing efficiency, we employed a cellular editing assay with a plasmid expressing human *pri-mir-376a2*.[28,35] A decrease in editing efficiency could indicate that the *GRIA2* Q/R site is not 100% edited in the brains of affected individuals.

Table 2. Characteristics of *ADARB1* Mutants Identified by Exome Sequencing in Affected Individuals

	Individual 1		Individual 2	Individual 3	Individual 4
	Variant 1	**Variant 2**			
Chromosome position (hg19)	chr21: 46602522G>C	chr21: 46604484A>G	chr21: 46595995A>G	chr21: 46624592G>A	chr21: 46642051C>T
cDNA change (GenBank: NM_015833.3)	c.1101G>C	c.1492A>G	c.379A>G	c.1808G>A	c.2165C>T
Amino acid change	p.Lys367Asn	p.Thr498Ala	p.Lys127Glu	p.Arg603Gln	p.Ala722Val
Inheritance	paternal	maternal	biparental (homozygous)	biparental (homozygous)	biparental (homozygous)
NCBI reference SNP number	rs778818769	rs544025652	N/A	rs1364071684	rs1323703791
***In silico* assessments**					
FATHMM	tolerated (1.41)	tolerated (1.63)	damaging (−2.33)	damaging (−4.34)	damaging (−3.35)
MutationAssessor	low (1.385)	neutral (−0.55)	high (4.745)	medium (3.465)	medium (3.11)
MutationTaster	disease causing	polymorphism	disease causing	disease causing	disease causing
PolyPhen2	benign (0.286)	benign (0)	probably damaging (1.00)	probably damaging (1.00)	possibly damaging (0.948)
SIFT	damaging	tolerated	damaging	damaging	damaging
PROVEAN	neutral	neutral	deleterious	deleterious	deleterious
CADD	23.1	0.174	25.9	33	29.3
GERP	1.53	−0.77	5.24	4.77	5.05
Disease Database					
epi25	not observed	not observed	not observed	not observed	not observed
Population Databases					
EVS	not observed	not observed	not observed	not observed	not observed
1000G	not observed	not observed	not observed	not observed	not observed
ExAC	not observed	1/1172 (no homozygotes)	not observed	not observed	not observed
gnomAD	2/235014 (8.510^{-6}); no homozygotes	47/88638 (5.3×10^{-4}); no homozygotes	not observed	1/251444 (3.98×10^{-6}); no homozygotes	1/245374 (4.08×10^{-6}); no homozygotes
Iranome	not observed	not observed	not observed	not observed	not observed
Other pathogenic or likely pathogenic variants associated with microcephaly, seizures, or intellectual disability in humans	not observed	not observed	not observed	not observed	not observed

HEK293T cells have very low endogenous ADAR2 RNA editing activity, which allows editing assays to be performed in this cell line with transiently expressed ADAR2.[28,36] Plasmids expressing FLAG-tagged ADAR2 mutant or wild-type enzymes were co-transfected into HEK293T cells with the *pri-mir-376a2*-expressing plasmid, and after 3 days, RNA was extracted from the cells. To ensure that ADAR2 concentrations were approximately the same in all samples, we used whole-cell lysates for immunoblotting and probed them with anti-FLAG antibody (Figures 3D and S2). RNA was treated with DNase1 prior to real-time PCR, and PCR products were Sanger sequenced. We assessed the editing efficiency by calculating the ratio of the guanosine peak height to the sum of adenosine and guanosine peak heights [G/(A+G)] at the editing site +4 of mir-376a2. The peak heights of the chromatograms at this editing site were measured with the QSVanalyser program.

As expected, four out of five variants caused a decrease in the editing activity of ADAR2 (Figures 3A and 3B). The p.Lys127Glu, p.Lys367Asn, and p.Ala722Val variants caused mild decreases in editing activity (14.6%, 10.9%, and 4.4% in ADAR2S, respectively), whereas the p.Arg603Gln variant resulted in a severe drop in editing activity (>85% decrease). Note that the severely reduced editing activity of the p.Arg603Gln variant is indistinguishable from background editing in untransfected HEK293T cells. The effects of these variants on editing activity were assessed by comparison to the effects of wild-type protein, and the same trend can be observed in both ADAR2S and ADAR2L isoforms, except for the p.Thr498Ala variant, which is only present in the

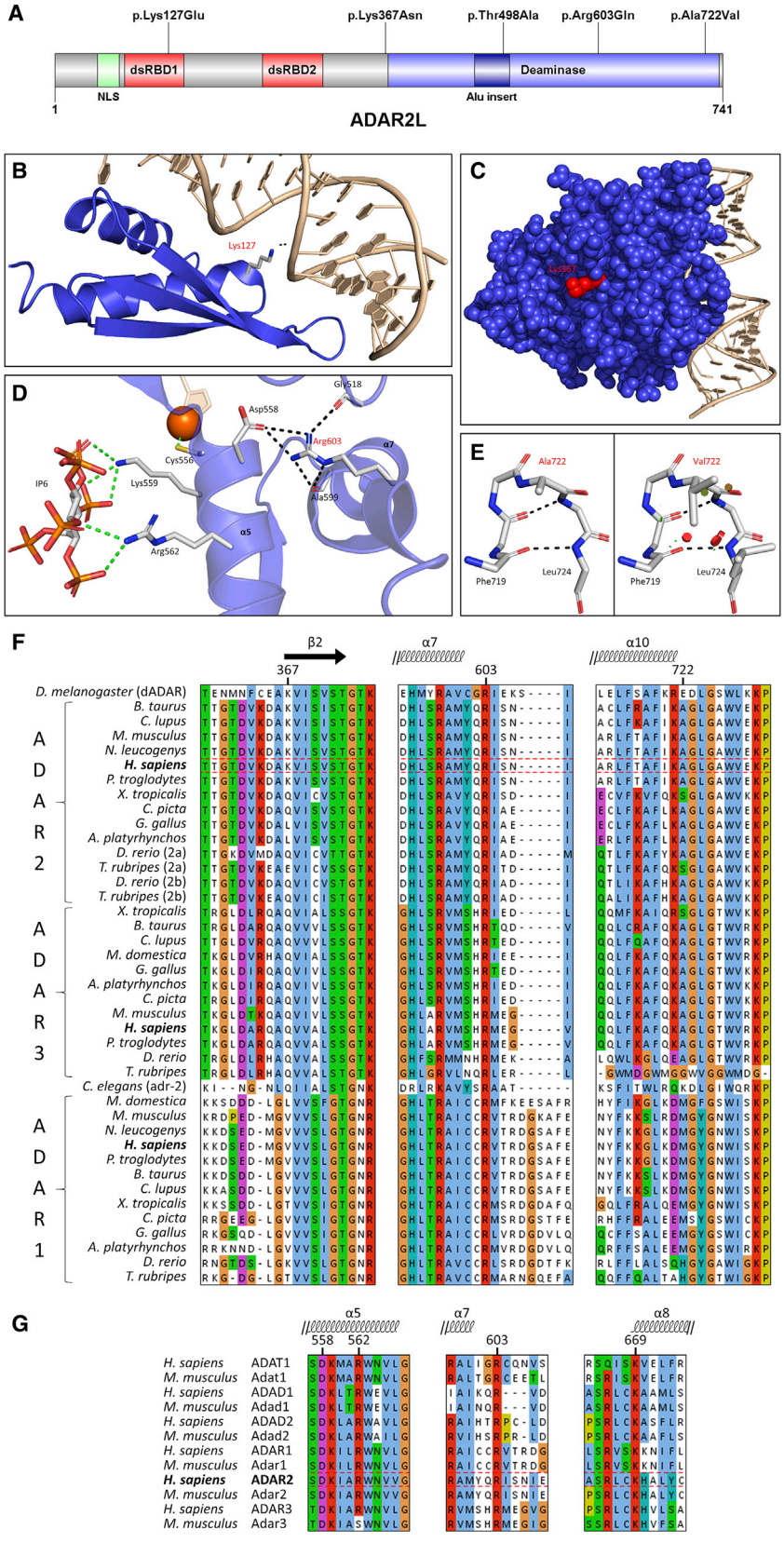

Figure 2. The Location and Conservation of *ADARB1* Variants

(A) Domain organization of ADAR2; locations of variants are indicated. NLS, nuclear localization signal.

(B) Cartoon model of ADAR2 dsRBD1 (blue). Lys127 makes contact with dsRNA (wheat) (PDB: 2L3C).

(C) Space-filling model of the ADAR2 deaminase domain (blue); Lys367 is highlighted in red (PDB: 5ED1).

(D) Close-up view of helices α5 and α7 of the ADAR2 deaminase domain (blue). The contacts made between Arg603 and other residues are represented as black dashed lines. Zinc coordination and interactions with IP6 are represented as green dashed lines. Zinc is illustrated as an orange sphere, IP6 is represented as a stick model (PDB: 5ED1).

(E) Stick model of the Schellman loop containing Ala722 (PDB ID: 5ED1). Hydrogen bonds are represented as black dashed lines. Only side chains of Ala722 (left) or Val722 and Leu724 (right) are shown. PyMOL Mutagenesis Wizard was used for replacing Ala722 with valine in the model. Val722 rotamer with the lowest strain is shown (right); unfavorable van der Waals overlaps are represented as colored disks.

(F and G) Multiple sequence alignments of ADAR1, ADAR2, and ADAR3 from diverse organisms (F) and of various related proteins containing the deaminase domain from human and mouse (G); locations of variants or other important residues are indicated above the alignments. Secondary structural elements observed in the ADAR2 deaminase domain are indicated. Human ADAR2 sequence is highlighted.

ADAR2L isoform. The decreases in editing efficiency with the p.Lys127Glu and p.Lys367Asn variants were more pronounced in the ADAR2S isoform than in the ADAR2L isoform. These results were further validated with an editing assay that employed a plasmid expressing the murine *Gria2* Q/R site RNA substrate (Figures 3C and S2).

The immunoblots demonstrate that the ADAR2 p.Arg603Gln recombinant protein attains low protein concentrations in transiently transfected cells (Figure 3D); such low protein concentrations were not observed with other ADAR2 variants (Figure S2). Furthermore, when protein synthesis was inhibited by cycloheximide, ADAR2 p.Arg603Gln protein concentrations decreased more rapidly than concentrations of ADAR2 wild-type protein (Figure 3E). These results indicated that the p.Arg603Gln variant affects the stability of ADAR2 protein.

Contrary to our expectations, the editing activity of the p.Thr498Ala mutant was not decreased (Figure 3B). Because ADAR2 forms a homodimer,[6,7] we investigated

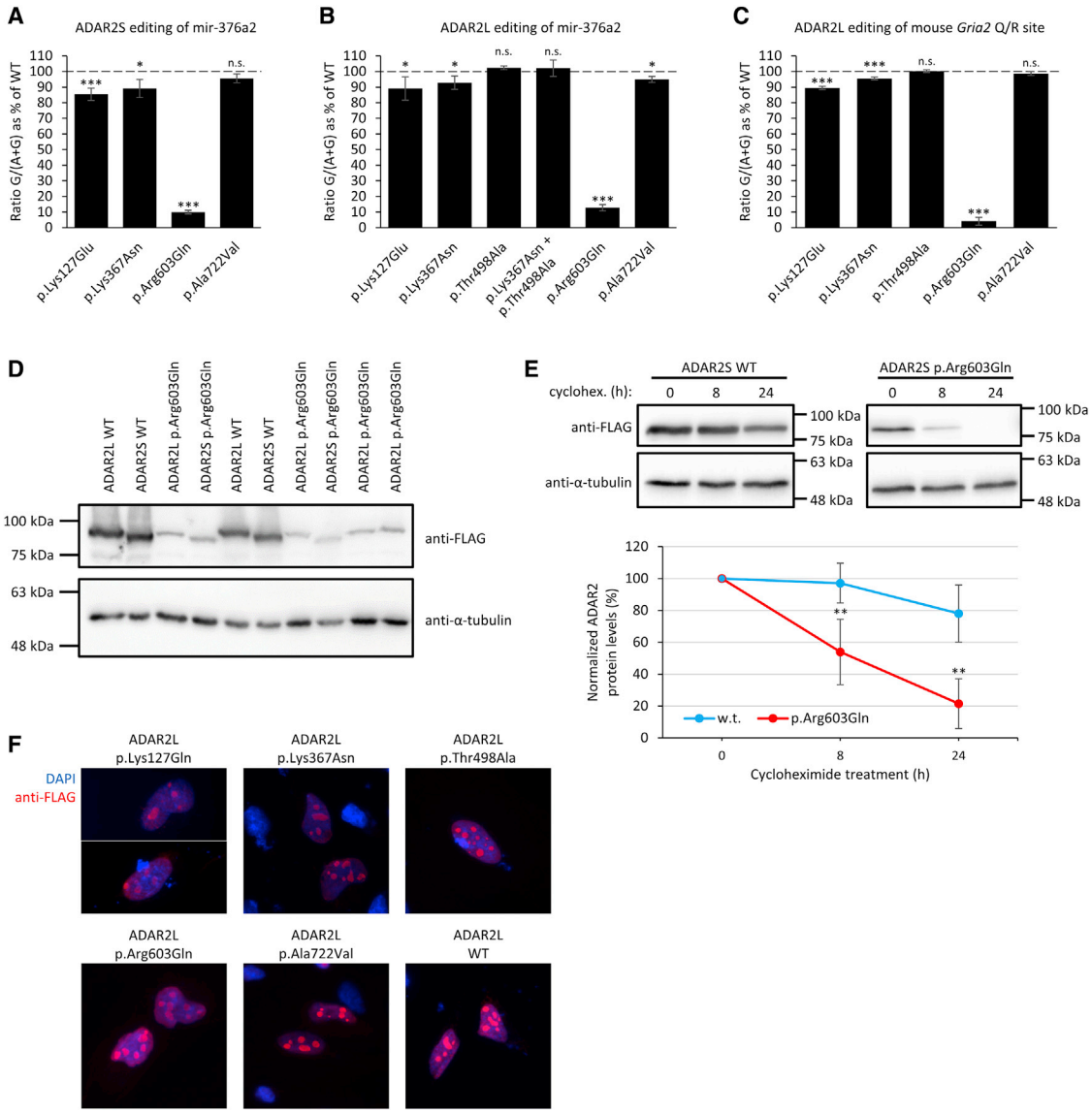

Figure 3. Editing Activity, Protein Stability, and Subcellular Localization of ADAR2 Variants

(A–C) Graphs showing editing at position +4 of human *pri-mir-376a2* by (A) ADAR2S or (B) ADAR2L in transiently transfected HEK293T cells and (C) graph showing editing at the mouse *Gria2* Q/R site by ADAR2L in transiently transfected HEK293T cells. G/(A+G) is the ratio of the guanosine peak height to the sum of adenosine and guanosine peak heights of the sequencing chromatograms. Editing levels were normalized to the editing by the wild-type protein, which is set as 100% (as indicated by a dashed line). Note that wild-type ADAR2L has lower editing efficiency (~70.6%) than wild-type ADAR2S (~74.5%). Data represent means ± SD ($n \geq 3$ independent experiments). *$p \leq 0.05$, **$p \leq 0.01$, and ***$p \leq 0.001$.

(D) Immunoblots probed with the indicated antibodies show protein amounts of FLAG-tagged wild-type ADAR2 or p.Arg603Gln proteins after co-transfection of HEK293T cells with plasmids expressing ADAR2 and *pri-mir-376a2*. Lanes with the same labels represent replicates.

(E) HEK293T cells transfected with FLAG-tagged wild-type ADAR2 or p.Arg603Gln were treated with cycloheximide (70 μg/mL) for the indicated times. Whole-cell lysates were used for immunoblotting with the indicated antibodies. Representative immunoblots are shown. Protein amounts were quantified by densitometric analysis of immunoblots. Data represent means ± SD ($n \geq 4$ independent experiments). *$p \leq 0.05$ and **$p \leq 0.01$.

(F) HeLa cells were transiently transfected with plasmids expressing the indicated FLAG-tagged proteins and analyzed by indirect immunofluorescence. Transfected cells were stained with anti-FLAG antibody (red channel). DAPI (blue channel) was used as a DNA stain. Cells with a representative staining pattern were selected.

the effect of the combination of p.Lys367Asn and p.Thr498Ala variants as seen in individual 1. To accomplish this, plasmids expressing ADAR2L mutants p.Lys367Asn and p.Thr498Ala were mixed in a 1:1 ratio and used in the same editing assay as above. The results again showed no decrease in editing activity compared to that of ADAR2L wild-type protein (Figure 3B). The results of the editing assay suggested that decreased editing activity might contribute to the phenotype, but only for four of the five variants, which

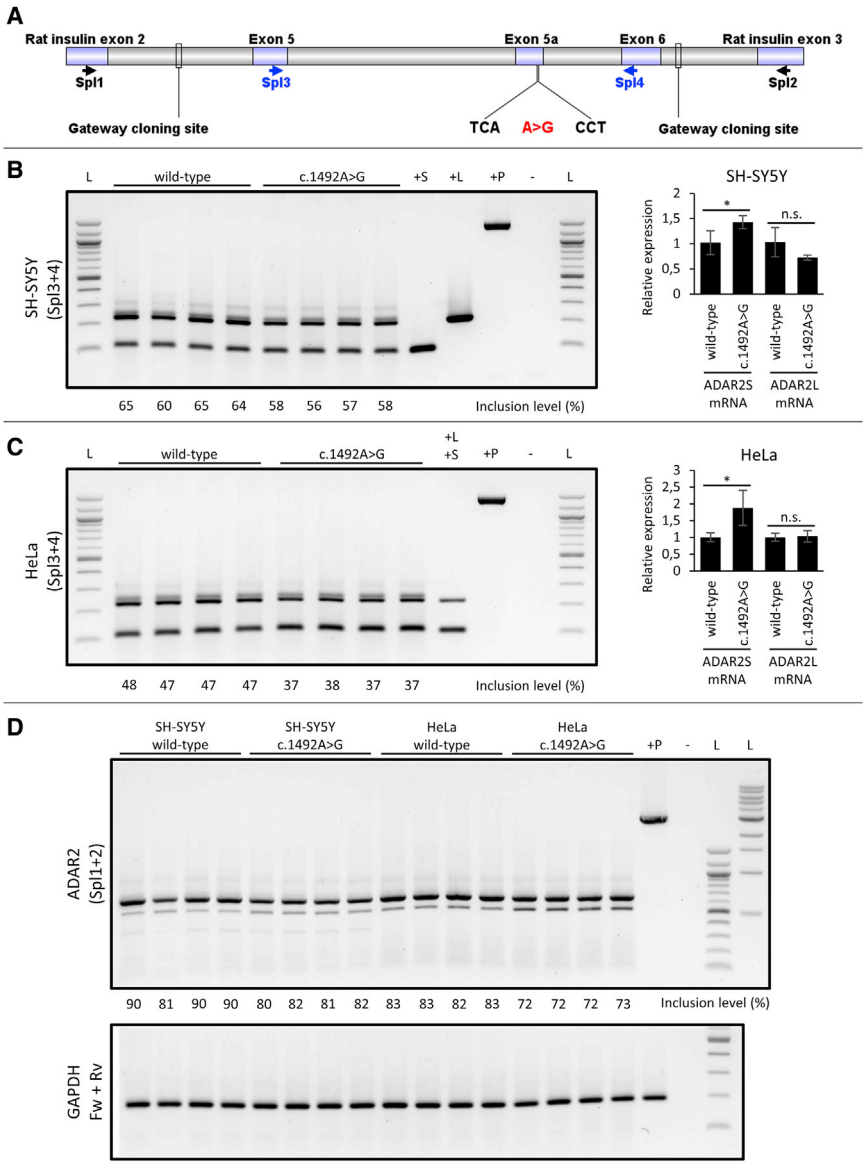

Figure 4. Splicing Effects of *ADARB1* c.1492A>G Variant

(A) Diagram depicting part of the *ADARB1* alternative exon 5a splicing reporter plasmid. An A-to-G variant that was found in individual 1 is shown in red and in the codon context. Primers used for PCR are represented by arrows below the exons.

(B–D) The wild-type or c.1492A>G splicing reporter plasmids were transfected into SH-SY5Y or HeLa cells, total RNA was isolated, real-time PCR was performed with the indicated primers, and splicing products were separated in 1% (Spl1+2) or 1.75% (Spl3+4, GAPDH) agarose gel (left panels). The *ADARB1* exon 5a inclusion level is calculated as a percentage of the total PCR products, i.e., 100% corresponds to the sum of the longer and shorter PCR products. +S, the *ADARB1* short-product positive control, and +L, the *ADARB1* long-product positive control, were generated directly from plasmids having these cDNA isoforms. +p, the *ADARB1* exon 5a fully unspliced positive control product, was also generated directly from the splicing-reporter-expressing plasmid. -, negative PCR control; L, 100 bp DNA ladder. qPCR was also performed with RNA from transiently transfected cells. qPCR results are normalized to mRNA expression in cells transfected with wild-type plasmid. Data represent means ± SD (n = 4 independent experiments). *p ≤ 0.05. (B) Analysis of splicing in transiently transfected SH-SY5Y cells by quantification of PCR bands on agarose gel (left) and by real-time qPCR quantification (right) (C). Analysis of splicing in transiently transfected HeLa cells by quantification of PCR bands on agarose gel (left) and by real-time qPCR quantification (right) (D). Confirmation of splicing analysis results by quantification of PCR bands on agarose gel with a different pair of primers (Spl1+Spl2). Note that the slightly larger band that migrates above the longer PCR product in (B) and (C) is a heteroduplex of shorter and longer PCR product (verified by Sanger sequencing).

led us to further investigate the effects of the p.Thr498Ala variant (see below).

The ADAR2 Variants Properly Localize to the Nucleoli

In the event that mislocalization of the ADAR2 mutants could contribute to the dysregulation of ADAR2, we analyzed the subcellular localization of all five ADAR2 variants. In this regard, the p.Lys127Glu variant is particularly interesting because it affects a critical lysine residue of dsRBD1. The mutation of this lysine to alanine in homologous domains of both human PKR and *Drosophila* Staufen was shown to result in a loss of dsRNA binding.[37,38] The RNA binding activity of ADAR2 was similarly affected when the residues Lys127 from dsRBD1 and Lys281 from dsRBD2 were both mutated to alanines.[39] Binding of dsRNA is required for nucleolar localization of ADAR2,[39] so we were interested in seeing whether the p.Lys127Glu variant would cause mislocalization of ADAR2.

HeLa cells were transiently transfected with plasmids expressing FLAG-tagged ADAR2 wild-type or mutant proteins, and indirect immunofluorescence with anti-FLAG antibody and DAPI staining was performed. The results show that all the tested variants in both ADAR2S and ADAR2L are localized in the nucleus (Figure 3F). Moreover, all the mutants are enriched in the nucleoli, as was previously reported for endogenous ADAR2.[39,40]

The c.1492A>G Variant Alters Splicing of Exon 5a

Given the location of the c.1492A>G (p.Thr498Ala) variant in the alternatively spliced exon 5a (Figure 4A), we investigated its impact on splicing. A minigene containing *ADARB1* exon 5a, the surrounding exons 5 and 6,

and parts of the flanking introns was cloned into the pDESTsplice[29] splicing reporter plasmid (Figure 4A). This construct was then transiently transfected into SH-SY5Y neuroblastoma cells and HeLa cells. These two cell lines were selected because they originate from different tissues, and we wanted to take into account the possible variability in the expression of splicing factors in different cell lines. 24 h after the transfection, we isolated total RNA and treated it with DNase, then performed real-time PCR to assess splicing of exon 5a with two different primer pairs (Figure 4A).

No difference in PCR band patterns between the wild-type and mutant minigene reporters was observed, indicating that the recognition of the 5′ splice site downstream of the c.1492A>G variant is not affected. However, the relative ratio of long (with exon 5a) and short (without exon 5a) PCR products, as measured by quantification of PCR bands on agarose gel, is shifted toward the short product in the mutant minigene reporter compared to the wild-type minigene reporter (Figures 4B–4D). The same trend was observed in SH-SY5Y and HeLa cells with both primer pairs. The relative decrease of mRNA containing exon 5a compared to the decrease of mRNA without exon 5a in the mutant minigene reporter was also confirmed by qPCR (Figures 4B and 4C). Thus, an effect of the c.1492A>G variant on alternative splicing of exon 5a was observed in the transfection experiment.

To check whether the c.1492A>G variant lies in an exonic splicing enhancer (ESE) or silencer region, we performed an *in silico* analysis with online algorithms that predict which sequences have the potential to bind splicing activators or repressors. We first tested the wild type and c.1492A>G mutant sequence of exon 5a with EX-SKIP and HOT-SKIP,[41] tools, which integrate several algorithms to determine which exonic variant has the highest chance of resulting in exon skipping. Both of these tools predict that the wild-type and c.1492A>G mutant exon 5a have a comparable chance of exon skipping. Next, we used ESEfinder 3.0[42,43] and SpliceAid 244 to look for differential binding of splicing activators and repressors. ESEfinder 3.0 predicts that the c.1492A>G variant creates a potential binding site for splicing factor SRSF1 (also known as SF2), whereas SpliceAid 2 predicts that the variant abolishes potential binding sites for NOVA1, NOVA2, and TRA2B (also known as Htra2-β1 or SFRS10) (Figure S3).

Real-Time qPCR Confirms an Increase in ADAR2S mRNA and a Decrease in the Inclusion of Exon 5a in Fibroblasts Derived from Individual 1

We used fibroblasts derived from individual 1 to measure *ADARB1* mRNA expression by real-time qPCR. Compared to fibroblasts from an age- and sex-matched control, individual 1's fibroblasts showed a very small increase in both total mRNA abundance and ADAR2S mRNA abundance. No change was observed in ADAR2L mRNA level (Figure 5A). Furthermore, ADAR2 protein concentration from control fibroblasts and individual 1's fibroblasts were assessed by immunoblot with anti-ADAR2 antibody, which demonstrated the same small increase in the concentration of ADAR2 in individual 1's fibroblasts (Figure 5B). The effect of the c.1492A>G variant on *ADARB1* mRNA splicing was also investigated by quantification of PCR products on agarose gels, which again revealed a decrease in exon 5a inclusion in individual 1's fibroblasts compared to control fibroblasts (Figure 5C). This experiment confirms the observation made with the splicing reporter. We made an attempt to directly investigate the editing activity of endogenous ADAR2 in these fibroblasts; however, the deaminase activity of ADAR2 in fibroblasts is very low. In addition, the transcript encoding the glutamate receptor subunit *GRIA2* is not expressed in fibroblasts, and transient transfection of plasmid expressing murine *Gria2* Q/R site did not lead to detectable editing in these cells (Figure S4).

Discussion

Herein we report human neurological disease associated with bi-allelic variants in *ADARB1*. The clinical phenotype comprises microcephaly, severe to profound developmental delay, hypotonia, and epilepsy that is largely intractable and, in one individual, is consistent clinically and electrographically with epilepsy of infancy with migrating focal seizures (EIMFS). Functional assays of four variants (p.Lys127Glu, p.Lys367Asn, p.Arg603Gln, and p.Ala722Val) demonstrate impairments in the RNA-editing ability of the resultant ADAR2 proteins, which are hypothesized to lead to increased Ca^{2+} permeability of AMPA receptors. Another variant, c.1492A>G (p.Thr498Ala), leads to a change in alternative splicing of the *ADARB1* gene to exclude exon 5a. These functional data support the pathogenic role of the *ADARB1* variants in the clinical phenotype observed in this cohort.

Diverse genes are involved in the pathogenesis of epileptic encephalopathies of infancy, and many of them encode proteins involved in synaptic functions and ion channels. Adding to this complexity, variants in the same gene can manifest as different epileptic syndromes (for review, see McTague et al.[44]). The epilepsy observed in individuals 2–4 is clinically consistent with an intractable epileptic encephalopathy, and the electrographic phenotype of individual 2 is consistent with EIMFS. Additional observations are needed to confirm *ADARB1* as a candidate for this intractable epilepsy syndrome alongside other causative genes.[45–56] More broadly, these data implicate *ADARB1* as a genetic etiology for early-onset epileptic encephalopathy, though additional milder epilepsy phenotypes might be possible.

The effects of ADAR2 on brain function have been comprehensively studied in mouse models.[57–59] Mice with total *Adar2* knockout have seizures and die within 3 weeks, but mice with single-allele *Adar2* knockout are

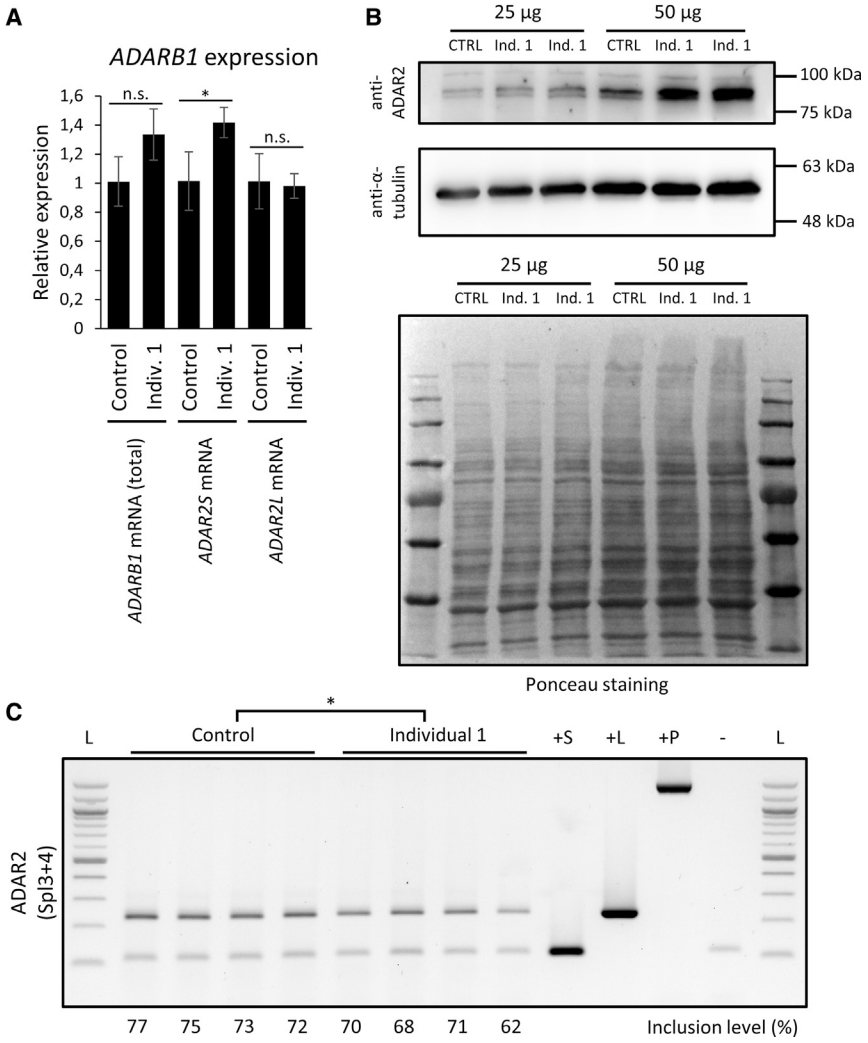

Figure 5. ADAR2 Expression and Splicing in Fibroblasts Derived from Individual 1

(A) Real-time qPCR analysis of short (ADAR2S), long (ADAR2L), and total ADAR2 mRNA isoforms in individual-1-derived and control fibroblasts. Results are normalized to mRNA expression in control fibroblasts. Data represent means ± SD (n = 4 independent experiments). *p ≤ 0.05.

(B) Immunoblots probed with indicated antibodies show protein levels of ADAR2 in individual-1-derived and control fibroblasts. Two total protein concentrations were loaded, and both α-tubulin and Ponceau staining were used as loading controls.

(C) Total RNA from individual-1-derived and control fibroblasts was used for real-time PCR and resolved on 1.75% agarose gel. The exon 5a inclusion level is calculated as a percentage of the longer PCR product, 100% corresponds to the sum of the longer and shorter PCR product. +S, short-product positive control; +L, long-product positive control; +p, wild-type-plasmid positive control; -, negative PCR control; and L, DNA ladder. *p ≤ 0.05.

phenotypically normal,[57] suggesting that a single functional allele of *Adar2* is sufficient for *Gria2* Q/R site editing and supporting the recessive inheritance pattern of *ADARB1* variants observed in this cohort. Furthermore, the importance of *GRIA2* Q/R-site editing for proper neuronal development was highlighted by a recent study reporting an individual with a *de novo* heterozygous variant, c.1819C>G (p.Gln607Glu), affecting the Q/R site of *GRIA2*.[22] This individual had an intractable epileptic encephalopathy with severe intellectual disability and limited functional capacity; this phenotype was similar to the one we observed in individuals 2–4 in this cohort. Functional studies of the *GRIA2* p.Gln607Glu variant demonstrated an increased current amplitude, which was hypothesized to explain the epilepsy in this individual. Because impaired Q/R site editing by ADAR2 variants in this cohort would be expected to result in increased AMPA receptor current as well, the phenotypic similarities among these individuals strengthen the conclusion that *ADARB1* variants cause the phenotype observed in this cohort.

The editing assay shows a mild decrease of the editing activity of the p.Lys127Glu variant located within the dsRBD1. Data from NMR structure of the dsRBDs of ADAR2 bound to dsRNA reveals that this amino acid makes non-sequence specific contacts with dsRNA.[31] It is part of a highly conserved motif present in dsRBDs, and when this entire motif is mutated, the binding to dsRNA is abolished.[37,38] Nucleolar localization of ADAR2 depends on binding to dsRNA,[39] but the p.Lys127Glu variant alone does not impair the localization of ADAR2 (Figure 3F). The unaffected dsRBD2 of the p.Lys127Glu variant probably compensates for its functional effect. However, on the basis of the NMR structure of the dsRBD bound to dsRNA, it is highly likely that the ability of the p.Lys127Glu variant to bind dsRNA is diminished. It should be noted that other RNA-binding proteins can compete with ADAR2 p.Lys127Glu for its natural targets, the full effect of which cannot be assessed in the *in vitro* assay because these proteins are not produced in HEK293T cells (such as ADAR3). Because RNA-binding proteins modulate the editing activity of ADARs,[60–63] we hypothesize that the *in vivo* effects of the p.Lys127Glu variant might be broader than what is reflected in the mild decrease of editing activity in our cell transfection assays.

The p.Lys367Asn variant has slightly decreased editing activity. According to the published structure of the ADAR2 deaminase domain (PDB ID: 5ED1),[32] the p.Lys367Asn variant lies at the surface of the protein on the side facing away from the edited RNA (Figure 2C). The affected residue is therefore accessible for potential protein-protein interactions, several of which have been

reported.[61,64–69] ADAR2 forms a homodimer,[3–7] but the residues involved in dimerization remain unknown. Determining whether some of these interactions could be impaired by the p.Lys367Asn variant will require further investigation of the ADAR2 interactome and the mechanism of ADAR2 dimerization.

The lack of knowledge about the structural role or the function of the 40-amino-acid-long ADAR2L-specific extension complicates the assessment of the effects of the p.Thr498Ala variant. We did not observe any decrease in the p.Thr498Ala mutant's editing activity; however, we cannot exclude the possibility that this variant might affect the editing of other targets. Because individual 1 is compound heterozygous for two variants in *ADARB1*, we also tested the editing activity of the p.Thr498Ala mutant in a co-transfection experiment with the p.Lys367Asn mutant and again observed no decrease in editing activity. Crystallographic studies of ADAR2S revealed that the region where the ADAR2L extension is located is disordered in the RNA-free state[70] but the end residues of this RNA-binding loop become ordered upon RNA binding.[32] The results of the splicing assay demonstrate that the c.1492A>G (p.Thr498Ala) variant has a small effect on the ratio of ADAR2S and ADAR2L splicing isoforms. The *in silico* analysis we performed highlights the possibility that the c.1492A>G variant causes differential binding of splicing regulators (SRSF1, NOVA1, NOVA2, and TRA2B). Others have shown that the co-transfection of a vector overexpressing SRSF1 with an ADAR2 wild-type minigene has no apparent effect on exon 5a inclusion.[71] TRA2B predominantly promotes exon inclusion by binding to ESE.[72,73] This is in line with the *in silico* analysis, which predicts that binding of TRA2B is impeded by the c.1492A>G variant. However, whether any of the proteins that are predicted to bind the affected sequence have a role in the alternative splicing of *ADARB1* exon 5a remains to be established.

Interestingly, we observed a change in the alternative splicing of the c.1492A>G mutant in favor of the more active ADAR2S isoform, suggesting that A-to-I editing would increase. However, without assessing alternative splicing of the c.1492A>G variant in developing neurons directly, we cannot draw a definitive conclusion about the effects of the c.1492A>G variant on alternative splicing in the human brain.

Notably, individual 1, who is compound heterozygous for the p.Lys367Asn and p.Thr498Ala variants, has a milder phenotype than the other individuals in this cohort. Fibroblasts from individual 1 might express slightly more ADAR2 protein than control fibroblasts (Figure 5B); this might compensate for reduced editing activity of the ADAR2 proteins in this individual. We hypothesize that this milder phenotype is related to an impact on an ADAR2 function that is editing independent, separate from its role in site-specific mRNA editing. Perhaps the alternative splicing seen in these assays disrupts critical protein-protein or protein-RNA interactions with other binding partners and thereby modifies other downstream targets important for neuronal function. Future studies on the editing-independent roles of ADAR2 will be important in elucidating these potential mechanisms. Ongoing clinical follow-up of individual 1 will be vital in assessing for evolution of his seizure phenotype or other neurological abnormalities. Reporting of other affected individuals with milder phenotypes associated with bi-allelic *ADARB1* variants will assist in drawing further genotype-phenotype correlations.

The results of the cycloheximide chase assay indicate that the p.Arg603Gln variant leads to faster degradation of ADAR2 (Figure 3E). One can explain the severe effects of this variant by examining the structure of the ADAR2 deaminase domain (PDB ID: 5ED1).[32] Arg603 interacts with Gly518, which is situated at the C-terminal end of the RNA-binding loop, and with Ala599, situated in helix α7 of the deaminase domain (Figure 2D). However, the most important interaction is with Asp558, situated in helix α5 of the deaminase domain. The zinc ligand residue Cys556 and IP6-interacting residues Lys559 and Arg562 are also located in helix α5. Thus, we expect that the p.Arg603Gln variant affects the folding and the stability of ADAR2 by altering the position of the catalytically important helix α5 and possibly by causing additional structural alterations in helix α7 and the RNA-binding loop.

The p.Ala722Val variant has a small effect on ADAR2 editing activity. This variant affects the Ccap residue of a Schellman loop that lies at the surface of the protein, close to the RNA-facing side of ADAR2 (Figure 2E). Alanine is one of the preferred amino acids at the Ccap position of a Schellman loop. On the other hand, valine at the Ccap was previously reported to be detrimental for the stability of the Schellman loop.[74] Besides affecting the editing activity as observed, this variant could additionally disrupt the local folding of ADAR2.

In summary, these findings suggest that the *ADARB1* variants detected in this cohort have multiple deleterious effects at both the RNA and protein levels and that these effects lead to microcephaly, intellectual disability, and epilepsy. The established importance of *GRIA2* Q/R site editing and its role in seizures in mouse models and humans lead us to hypothesize that the phenotypes observed in these individuals, particularly the epilepsy phenotype, are at least partially caused by *GRIA2* under-editing. However, we cannot exclude the possibility that ADAR2 plays other roles, mediated by protein-protein or protein-RNA interactions, in the disease.

Supplemental Data

Supplemental Data can be found online at https://doi.org/10.1016/j.ajhg.2020.02.015.

Acknowledgments

We acknowledge the Core Facility Cellular Imaging (CELLIM) of Central European Institute of Technology (CEITEC) supported

by the Czech-BioImaging large RI project (LM2015062 funded by the Ministry of Education Youth and Sports Czech Republic (MEYS CR)), for support with obtaining scientific data presented in this paper. W.K.C. was funded by grants from the Simons Foundation Autism Research Initiative (SFARI) and the JPB Foundation. This work was supported by the European Union's Seventh Framework Programme for research, technological development, and demonstration under grant agreement number 621368 to M.A.O. L.P.K. has received funding from Czech Science Foundation project number 19-16963S. The research conducted at the Murdoch Children's Research Institute was supported by the Victorian Government's Operational Infrastructure Support Program. Sequencing and analysis of individual 1 were provided by the Broad Institute of MIT and Harvard Center for Mendelian Genomics (Broad CMG) and were funded by the National Human Genome Research Institute, the National Eye Institute, and the National Heart, Lung, and Blood Institute under grant UM1 HG008900 to Daniel MacArthur and Heidi Rehm.

Declaration of Interests

J.J. is an employee of GeneDx, Inc. All other authors declare no competing interests.

Received: November 12, 2019
Accepted: February 26, 2020
Published: March 26, 2020

Web Resources

1000 Genomes Project, https://www.internationalgenome.org/
Combined Annotation Dependent Depletion (CADD), https://cadd.gs.washington.edu/
Epi25 database, http://epi25.broadinstitute.org/
Exome Variant Server (EVS), https://evs.gs.washington.edu/EVS/
Functional Analysis through Hidden Markov Models, http://fathmm.biocompute.org.uk/
GeneMatcher, https://genematcher.org/
GeneReviews, McTague A., and Kurian M.A. (1993). SLC12A5-Related Epilepsy of Infancy with Migrating Focal Seizures. https://www.ncbi.nlm.nih.gov/pubmed/30763027
Genomic Evolutionary Rate Profiling (GERP), http://mendel.stanford.edu/SidowLab/downloads/gerp/
Genome Aggregation Database (GnomAD), https://gnomad.broadinstitute.org/
Iranome, http://www.iranome.ir/
Matchmaker Exchange, https://www.matchmakerexchange.org
Mutation Assessor, http://mutationassessor.org/
Mutation Taster, http://www.mutationtaster.org/
Online Mendelian Inheritance in Man, http://www.omim.org
PolyPhen2, http://genetics.bwh.harvard.edu/pph2/
Protein Variation Effect Analyzer (PROVEAN), http://provean.jcvi.org/index.php
Sorting Intolerant from Tolerant (SIFT), https://sift.bii.a-star.edu.sg/

References

1. Sinigaglia, K., Wiatrek, D., Khan, A., Michalik, D., Sambrani, N., Sedmík, J., Vukić, D., O'Connell, M.A., and Keegan, L.P. (2019). ADAR RNA editing in innate immune response phasing, in circadian clocks and in sleep. Biochim. Biophys. Acta. Gene Regul. Mech. *1862*, 356–369.
2. Licht, K., Hartl, M., Amman, F., Anrather, D., Janisiw, M.P., and Jantsch, M.F. (2019). Inosine induces context-dependent recoding and translational stalling. Nucleic Acids Res. *47*, 3–14.
3. Jaikaran, D.C., Collins, C.H., and MacMillan, A.M. (2002). Adenosine to inosine editing by ADAR2 requires formation of a ternary complex on the GluR-B R/G site. J. Biol. Chem. *277*, 37624–37629.
4. Poulsen, H., Jorgensen, R., Heding, A., Nielsen, F.C., Bonven, B., and Egebjerg, J. (2006). Dimerization of ADAR2 is mediated by the double-stranded RNA binding domain. RNA *12*, 1350–1360.
5. Chilibeck, K.A., Wu, T., Liang, C., Schellenberg, M.J., Gesner, E.M., Lynch, J.M., and MacMillan, A.M. (2006). FRET analysis of in vivo dimerization by RNA-editing enzymes. J. Biol. Chem. *281*, 16530–16535.
6. Valente, L., and Nishikura, K. (2007). RNA binding-independent dimerization of adenosine deaminases acting on RNA and dominant negative effects of nonfunctional subunits on dimer functions. J. Biol. Chem. *282*, 16054–16061.
7. Gallo, A., Keegan, L.P., Ring, G.M., and O'Connell, M.A. (2003). An ADAR that edits transcripts encoding ion channel subunits functions as a dimer. EMBO J. *22*, 3421–3430.
8. Rice, G.I., Kasher, P.R., Forte, G.M., Mannion, N.M., Greenwood, S.M., Szynkiewicz, M., Dickerson, J.E., Bhaskar, S.S., Zampini, M., Briggs, T.A., et al. (2012). Mutations in ADAR1 cause Aicardi-Goutières syndrome associated with a type I interferon signature. Nat. Genet. *44*, 1243–1248.
9. Livingston, J.H., Lin, J.P., Dale, R.C., Gill, D., Brogan, P., Munnich, A., Kurian, M.A., Gonzalez-Martinez, V., De Goede, C.G., Falconer, A., et al. (2014). A type I interferon signature identifies bilateral striatal necrosis due to mutations in ADAR1. J. Med. Genet. *51*, 76–82.
10. Miyamura, Y., Suzuki, T., Kono, M., Inagaki, K., Ito, S., Suzuki, N., and Tomita, Y. (2003). Mutations of the RNA-specific adenosine deaminase gene (DSRAD) are involved in dyschromatosis symmetrica hereditaria. Am. J. Hum. Genet. *73*, 693–699.
11. Kondo, T., Suzuki, T., Ito, S., Kono, M., Negoro, T., and Tomita, Y. (2008). Dyschromatosis symmetrica hereditaria associated with neurological disorders. J. Dermatol. *35*, 662–666.
12. Tojo, K., Sekijima, Y., Suzuki, T., Suzuki, N., Tomita, Y., Yoshida, K., Hashimoto, T., and Ikeda, S. (2006). Dystonia, mental deterioration, and dyschromatosis symmetrica hereditaria in a family with ADAR1 mutation. Mov. Disord. *21*, 1510–1513.
13. Aizawa, H., Sawada, J., Hideyama, T., Yamashita, T., Katayama, T., Hasebe, N., Kimura, T., Yahara, O., and Kwak, S. (2010). TDP-43 pathology in sporadic ALS occurs in motor neurons lacking the RNA editing enzyme ADAR2. Acta Neuropathol. *120*, 75–84.
14. Kawahara, Y., Ito, K., Ito, M., Tsuji, S., and Kwak, S. (2005). Novel splice variants of human ADAR2 mRNA: skipping of the exon encoding the dsRNA-binding domains, and multiple C-terminal splice sites. Gene *363*, 193–201.
15. Gerber, A., O'Connell, M.A., and Keller, W. (1997). Two forms of human double-stranded RNA-specific editase 1 (hRED1) generated by the insertion of an Alu cassette. RNA *3*, 453–463.
16. Lai, F., Chen, C.X., Carter, K.C., and Nishikura, K. (1997). Editing of glutamate receptor B subunit ion channel RNAs by four alternatively spliced DRADA2 double-stranded RNA adenosine deaminases. Mol. Cell. Biol. *17*, 2413–2424.

17. Filippini, A., Bonini, D., Giacopuzzi, E., La Via, L., Gangemi, F., Colombi, M., and Barbon, A. (2018). Differential Enzymatic Activity of Rat ADAR2 Splicing Variants Is Due to Altered Capability to Interact with RNA in the Deaminase Domain. Genes (Basel) *9*, E79.
18. Tan, M.H., Li, Q., Shanmugam, R., Piskol, R., Kohler, J., Young, A.N., et al. (2017). Dynamic landscape and regulation of RNA editing in mammals. Nature *550*, 249–254.
19. Sommer, B., Köhler, M., Sprengel, R., and Seeburg, P.H. (1991). RNA editing in brain controls a determinant of ion flow in glutamate-gated channels. Cell *67*, 11–19.
20. Greger, I.H., Khatri, L., Kong, X., and Ziff, E.B. (2003). AMPA receptor tetramerization is mediated by Q/R editing. Neuron *40*, 763–774.
21. Greger, I.H., Khatri, L., and Ziff, E.B. (2002). RNA editing at arg607 controls AMPA receptor exit from the endoplasmic reticulum. Neuron *34*, 759–772.
22. Salpietro, V., Dixon, C.L., Guo, H., Bello, O.D., Vandrovcova, J., Efthymiou, S., Maroofian, R., Heimer, G., Burglen, L., Valence, S., et al.; SYNAPS Study Group (2019). AMPA receptor GluA2 subunit defects are a cause of neurodevelopmental disorders. Nat. Commun. *10*, 3094.
23. Slavov, D., and Gardiner, K. (2002). Phylogenetic comparison of the pre-mRNA adenosine deaminase ADAR2 genes and transcripts: conservation and diversity in editing site sequence and alternative splicing patterns. Gene *299*, 83–94.
24. Philippakis, A.A., Azzariti, D.R., Beltran, S., Brookes, A.J., Brownstein, C.A., Brudno, M., Brunner, H.G., Buske, O.J., Carey, K., Doll, C., et al. (2015). The Matchmaker Exchange: a platform for rare disease gene discovery. Hum. Mutat. *36*, 915–921.
25. Sobreira, N., Schiettecatte, F., Valle, D., and Hamosh, A. (2015). GeneMatcher: a matching tool for connecting investigators with an interest in the same gene. Hum. Mutat. *36*, 928–930.
26. Retterer, K., Juusola, J., Cho, M.T., Vitazka, P., Millan, F., Gibellini, F., Vertino-Bell, A., Smaoui, N., Neidich, J., Monaghan, K.G., et al. (2016). Clinical application of whole-exome sequencing across clinical indications. Genet. Med. *18*, 696–704.
27. Zhu, N., Gonzaga-Jauregui, C., Welch, C.L., Ma, L., Qi, H., King, A.K., Krishnan, U., Rosenzweig, E.B., Ivy, D.D., Austin, E.D., et al. (2018). Exome Sequencing in Children With Pulmonary Arterial Hypertension Demonstrates Differences Compared With Adults. Circ Genom Precis Med *11*, e001887.
28. Heale, B.S., Keegan, L.P., McGurk, L., Michlewski, G., Brindle, J., Stanton, C.M., Caceres, J.F., and O'Connell, M.A. (2009). Editing independent effects of ADARs on the miRNA/siRNA pathways. EMBO J. *28*, 3145–3156.
29. Kishore, S., Khanna, A., and Stamm, S. (2008). Rapid generation of splicing reporters with pSpliceExpress. Gene *427*, 104–110.
30. Livak, K.J., and Schmittgen, T.D. (2001). Analysis of relative gene expression data using real-time quantitative PCR and the 2(-Delta Delta C(T)) Method. Methods *25*, 402–408.
31. Stefl, R., Oberstrass, F.C., Hood, J.L., Jourdan, M., Zimmermann, M., Skrisovska, L., Maris, C., Peng, L., Hofr, C., Emeson, R.B., and Allain, F.H. (2010). The solution structure of the ADAR2 dsRBM-RNA complex reveals a sequence-specific readout of the minor groove. Cell *143*, 225–237.
32. Matthews, M.M., Thomas, J.M., Zheng, Y., Tran, K., Phelps, K.J., Scott, A.I., Havel, J., Fisher, A.J., and Beal, P.A. (2016). Structures of human ADAR2 bound to dsRNA reveal base-flipping mechanism and basis for site selectivity. Nat. Struct. Mol. Biol. *23*, 426–433.
33. Aurora, R., Srinivasan, R., and Rose, G.D. (1994). Rules for alpha-helix termination by glycine. Science *264*, 1126–1130.
34. Masliah, G., Barraud, P., and Allain, F.H. (2013). RNA recognition by double-stranded RNA binding domains: a matter of shape and sequence. Cell. Mol. Life Sci. *70*, 1875–1895.
35. Mannion, N.M., Greenwood, S.M., Young, R., Cox, S., Brindle, J., Read, D., Nellåker, C., Vesely, C., Ponting, C.P., McLaughlin, P.J., et al. (2014). The RNA-editing enzyme ADAR1 controls innate immune responses to RNA. Cell Rep. *9*, 1482–1494.
36. Daniel, C., Widmark, A., Rigardt, D., and Öhman, M. (2017). Editing inducer elements increases A-to-I editing efficiency in the mammalian transcriptome. Genome Biol. *18*, 195.
37. McMillan, N.A., Carpick, B.W., Hollis, B., Toone, W.M., Zamanian-Daryoush, M., and Williams, B.R. (1995). Mutational analysis of the double-stranded RNA (dsRNA) binding domain of the dsRNA-activated protein kinase, PKR. J. Biol. Chem. *270*, 2601–2606.
38. Ramos, A., Grünert, S., Adams, J., Micklem, D.R., Proctor, M.R., Freund, S., Bycroft, M., St Johnston, D., and Varani, G. (2000). RNA recognition by a Staufen double-stranded RNA-binding domain. EMBO J. *19*, 997–1009.
39. Sansam, C.L., Wells, K.S., and Emeson, R.B. (2003). Modulation of RNA editing by functional nucleolar sequestration of ADAR2. Proc. Natl. Acad. Sci. USA *100*, 14018–14023.
40. Desterro, J.M.P., Keegan, L.P., Lafarga, M., Berciano, M.T., O'Connell, M., and Carmo-Fonseca, M. (2003). Dynamic association of RNA-editing enzymes with the nucleolus. J. Cell Sci. *116*, 1805–1818.
41. Raponi, M., Kralovicova, J., Copson, E., Divina, P., Eccles, D., Johnson, P., Baralle, D., and Vorechovsky, I. (2011). Prediction of single-nucleotide substitutions that result in exon skipping: identification of a splicing silencer in BRCA1 exon 6. Hum. Mutat. *32*, 436–444.
42. Cartegni, L., Wang, J., Zhu, Z., Zhang, M.Q., and Krainer, A.R. (2003). ESEfinder: A web resource to identify exonic splicing enhancers. Nucleic Acids Res. *31*, 3568–3571.
43. Smith, P.J., Zhang, C., Wang, J., Chew, S.L., Zhang, M.Q., and Krainer, A.R. (2006). An increased specificity score matrix for the prediction of SF2/ASF-specific exonic splicing enhancers. Hum. Mol. Genet. *15*, 2490–2508.
44. McTague, A., Howell, K.B., Cross, J.H., Kurian, M.A., and Scheffer, I.E. (2016). The genetic landscape of the epileptic encephalopathies of infancy and childhood. Lancet Neurol. *15*, 304–316.
45. Ambrosino, P., Soldovieri, M.V., Bast, T., Turnpenny, P.D., Uhrig, S., Biskup, S., Döcker, M., Fleck, T., Mosca, I., Manocchio, L., et al. (2018). De novo gain-of-function variants in KCNT2 as a novel cause of developmental and epileptic encephalopathy. Ann. Neurol. *83*, 1198–1204.
46. Duan, H., Peng, J., Kessi, M., and Yin, F. (2018). De Novo KCNQ2 Mutation in One Case of Epilepsy of Infancy With Migrating Focal Seizures That Evolved to Infantile Spasms. Child Neurol. Open *5*, X18767738.
47. Freibauer, A., and Jones, K. (2018). KCNQ2 mutation in an infant with encephalopathy of infancy with migrating focal seizures. Epileptic Disord. *20*, 541–544.
48. Freilich, E.R., Jones, J.M., Gaillard, W.D., Conry, J.A., Tsuchida, T.N., Reyes, C., Dib-Hajj, S., Waxman, S.G., Meisler, M.H., and Pearl, P.L. (2011). Novel SCN1A mutation in a proband with

malignant migrating partial seizures of infancy. Arch. Neurol. *68*, 665–671.
49. Gorman, K.M., Forman, E., Conroy, J., Allen, N.M., Shahwan, A., Lynch, S.A., Ennis, S., and King, M.D. (2017). Novel SMC1A variant and epilepsy of infancy with migrating focal seizures: Expansion of the phenotype. Epilepsia *58*, 1301–1302.
50. Howell, K.B., McMahon, J.M., Carvill, G.L., Tambunan, D., Mackay, M.T., Rodriguez-Casero, V., Webster, R., Clark, D., Freeman, J.L., Calvert, S., et al. (2015). SCN2A encephalopathy: A major cause of epilepsy of infancy with migrating focal seizures. Neurology *85*, 958–966.
51. Komulainen-Ebrahim, J., Schreiber, J.M., Kangas, S.M., Pylkäs, K., Suo-Palosaari, M., Rahikkala, E., Liinamaa, J., Immonen, E.V., Hassinen, I., Myllynen, P., et al. (2019). Novel variants and phenotypes widen the phenotypic spectrum of GABRG2-related disorders. Seizure *69*, 99–104.
52. Poduri, A., Heinzen, E.L., Chitsazzadeh, V., Lasorsa, F.M., Elhosary, P.C., LaCoursiere, C.M., Martin, E., Yuskaitis, C.J., Hill, R.S., Atabay, K.D., et al. (2013). SLC25A22 is a novel gene for migrating partial seizures in infancy. Ann. Neurol. *74*, 873–882.
53. Rizzo, F., Ambrosino, P., Guacci, A., Chetta, M., Marchese, G., Rocco, T., Soldovieri, M.V., Manocchio, L., Mosca, I., Casara, G., et al. (2016). Characterization of two de novoKCNT1 mutations in children with malignant migrating partial seizures in infancy. Mol. Cell. Neurosci. *72*, 54–63.
54. Štěrbová, K., Vlčková, M., Klement, P., Neupauerová, J., Staněk, D., Zůnová, H., Seeman, P., and Laššuthová, P. (2018). Neonatal Onset of Epilepsy of Infancy with Migrating Focal Seizures Associated with a Novel GABRB3 Variant in Monozygotic Twins. Neuropediatrics *49*, 204–208.
55. Stödberg, T., McTague, A., Ruiz, A.J., Hirata, H., Zhen, J., Long, P., Farabella, I., Meyer, E., Kawahara, A., Vassallo, G., et al. (2015). Mutations in SLC12A5 in epilepsy of infancy with migrating focal seizures. Nat. Commun. *6*, 8038.
56. Su, D.J., Lu, J.F., Lin, L.J., Liang, J.S., and Hung, K.L. (2018). SCN2A mutation in an infant presenting with migrating focal seizures and infantile spasm responsive to a ketogenic diet. Brain Dev. *40*, 724–727.
57. Higuchi, M., Maas, S., Single, F.N., Hartner, J., Rozov, A., Burnashev, N., Feldmeyer, D., Sprengel, R., and Seeburg, P.H. (2000). Point mutation in an AMPA receptor gene rescues lethality in mice deficient in the RNA-editing enzyme ADAR2. Nature *406*, 78–81.
58. Jia, Z., Agopyan, N., Miu, P., Xiong, Z., Henderson, J., Gerlai, R., Taverna, F.A., Velumian, A., MacDonald, J., Carlen, P., et al. (1996). Enhanced LTP in mice deficient in the AMPA receptor GluR2. Neuron *17*, 945–956.
59. Brusa, R., Zimmermann, F., Koh, D.-S., Feldmeyer, D., Gass, P., Seeburg, P.H., and Sprengel, R. (1995). Early-onset epilepsy and postnatal lethality associated with an editing-deficient GluR-B allele in mice. Science *270*, 1677–1680.
60. Garncarz, W., Tariq, A., Handl, C., Pusch, O., and Jantsch, M.F. (2013). A high-throughput screen to identify enhancers of ADAR-mediated RNA-editing. RNA Biol. *10*, 192–204.
61. Tariq, A., Garncarz, W., Handl, C., Balik, A., Pusch, O., and Jantsch, M.F. (2013). RNA-interacting proteins act as site-specific repressors of ADAR2-mediated RNA editing and fluctuate upon neuronal stimulation. Nucleic Acids Res. *41*, 2581–2593.
62. Bratt, E., and Ohman, M. (2003). Coordination of editing and splicing of glutamate receptor pre-mRNA. RNA *9*, 309–318.
63. Quinones-Valdez, G., Tran, S.S., Jun, H.I., Bahn, J.H., Yang, E.W., Zhan, L., Brümmer, A., Wei, X., Van Nostrand, E.L., Pratt, G.A., et al. (2019). Regulation of RNA editing by RNA-binding proteins in human cells. Commun Biol *2*, 19.
64. Bhogal, B., Jepson, J.E., Savva, Y.A., Pepper, A.S., Reenan, R.A., and Jongens, T.A. (2011). Modulation of dADAR-dependent RNA editing by the Drosophila fragile X mental retardation protein. Nat. Neurosci. *14*, 1517–1524.
65. Filippini, A., Bonini, D., Lacoux, C., Pacini, L., Zingariello, M., Sancillo, L., Bosisio, D., Salvi, V., Mingardi, J., La Via, L., et al. (2017). Absence of the Fragile X Mental Retardation Protein results in defects of RNA editing of neuronal mRNAs in mouse. RNA Biol. *14*, 1580–1591.
66. Marcucci, R., Brindle, J., Paro, S., Casadio, A., Hempel, S., Morrice, N., Bisso, A., Keegan, L.P., Del Sal, G., and O'Connell, M.A. (2011). Pin1 and WWP2 regulate GluR2 Q/R site RNA editing by ADAR2 with opposing effects. EMBO J. *30*, 4211–4222.
67. Qi, L., Song, Y., Chan, T.H.M., Yang, H., Lin, C.H., Tay, D.J.T., Hong, H., Tang, S.J., Tan, K.T., Huang, X.X., et al. (2017). An RNA editing/dsRNA binding-independent gene regulatory mechanism of ADARs and its clinical implication in cancer. Nucleic Acids Res. *45*, 10436–10451.
68. Shamay-Ramot, A., Khermesh, K., Porath, H.T., Barak, M., Pinto, Y., Wachtel, C., Zilberberg, A., Lerer-Goldshtein, T., Efroni, S., Levanon, E.Y., and Appelbaum, L. (2015). Fmrp Interacts with Adar and Regulates RNA Editing, Synaptic Density and Locomotor Activity in Zebrafish. PLoS Genet. *11*, e1005702.
69. Shelton, P.M., Duran, A., Nakanishi, Y., Reina-Campos, M., Kasashima, H., Llado, V., Ma, L., Campos, A., García-Olmo, D., García-Arranz, M., et al. (2018). The Secretion of miR-200s by a PKCζ/ADAR2 Signaling Axis Promotes Liver Metastasis in Colorectal Cancer. Cell Rep. *23*, 1178–1191.
70. Macbeth, M.R., Schubert, H.L., Vandemark, A.P., Lingam, A.T., Hill, C.P., and Bass, B.L. (2005). Inositol hexakisphosphate is bound in the ADAR2 core and required for RNA editing. Science *309*, 1534–1539.
71. Sorek, R., Lev-Maor, G., Reznik, M., Dagan, T., Belinky, F., Graur, D., and Ast, G. (2004). Minimal conditions for exonization of intronic sequences: 5′ splice site formation in alu exons. Mol. Cell *14*, 221–231.
72. Dichmann, D.S., Walentek, P., and Harland, R.M. (2015). The alternative splicing regulator Tra2b is required for somitogenesis and regulates splicing of an inhibitory Wnt11b isoform. Cell Rep. *10*, 527–536.
73. Storbeck, M., Hupperich, K., Gaspar, J.A., Meganathan, K., Martínez Carrera, L., Wirth, R., Sachinidis, A., and Wirth, B. (2014). Neuronal-specific deficiency of the splicing factor Tra2b causes apoptosis in neurogenic areas of the developing mouse brain. PLoS ONE *9*, e89020.
74. Newell, N.E. (2011). Cascade detection for the extraction of localized sequence features; specificity results for HIV-1 protease and structure-function results for the Schellman loop. Bioinformatics *27*, 3415–3422.